Amplitude Modulation of de Haas–van Alphen Waveforms*

H. Alles† and D. H. Lowndes
Department of Physics, University of Oregon, Eugene, Oregon 97403
(Received 31 May 1973)

We report detailed experimental measurements and calculations of the amplitude modulation (AM) of a high-frequency de Haas-van Alphen (dHvA) quantum-oscillation waveform, due to magnetic interaction with a low-frequency dHvA oscillation. Experiments were carried out using a pure Au single crystal with H parallel to the ⟨111⟩ direction, at 36.1 kG and 2.0 K. Two new mechanisms by which AM can arise are described in detail: (i) AM can arise in conjunction with the frequency modulation (FM) due to magnetic interaction, through modulation of the Bessel-function arguments which appear in using the field-modulation technique. This FM-AM effect is an unavoidable consequence of using the field-modulation technique in the presence of magnetic interaction. The resulting AM waveforms can be totally different in appearance at different detection harmonics. (ii) AM can also arise via magnetic interaction and phase smearing in an inhomogeneous magnetic field. The observed AM, as a function of a linear magnetic field gradient, is in good qualitative agreement with the prediction of Hornfeldt, Ketterson, and Windmiller. Possible applications of AM effects are briefly discussed.

I. INTRODUCTION

Measurements of the magnetic field dependence of the *amplitude* of de Haas-van Alphen (dHvA) quantum oscillations have, in the past several years, become a prime source of information regarding the anisotropy of conduction-electron scattering rates at different points (or regions) on the Fermi surface.[1-9] The resulting maps, showing the variation of the electronic-scattering rate over the Fermi surface, are being applied to obtain a better theoretical understanding of the effect of electronic-lifetime anisotropy on the transport properties of metals and dilute alloys.[1,2,4,5,7-9] Experiments have been carried out so far for scattering by controlled amounts of lattice defects such as dislocations,[6] but mainly for dilute alloys, for which the electronic scattering rate is dominated by the effects of random substitutional impurities. The most detailed studies have been made for alloys based on noble-metal (Cu, Ag, Au) hosts, and containing up to several tenths of an atomic percent of various solute atoms.[1,2,7,8]

Since these determinations of electronic lifetime anisotropy depend on accurate measurements of the amplitudes of dHvA oscillations, it is particularly important to fully understand all effects, spurious or fundamental, which produce departures from the Lifshitz-Kosevitch expression for the dHvA amplitude. Some of the stringent experimental conditions required for accurate measurements of dHvA *amplitudes* are now well known.[10] Magnetic field inhomogeneity, mosaic spread in microcrystalline orientation, and inhomogeneous solute distribution can all cause spurious (and magnetic-field-*dependent*) reductions in the dHvA amplitude A, via phase smearing, with consequent errors in the electron-scattering rates determined from "Dingle plots" of $\ln(AH^{1/2})$ vs $(1/H)$.[1,2] Similarly, the self-magnetic-interaction (MI) effect distorts the waveform of a dHvA oscillation,[11] generally changing its fundamental amplitude slightly and drastically increasing its harmonic content.[12] These effects are largest when $a = 4\pi(\partial M/\partial H) > 1$ (strong MI limit) and so MI has been studied mainly in pure metals at low temperatures, in order to achieve this condition.

However, strongly *amplitude-modulated* (AM) waveforms are also commonly found when the dHvA effect is observed at crystal orientations for which both a high-frequency and a low-frequency oscillation are present. For example, with H along the ⟨111⟩ direction in a noble metal, the high-frequency belly (F_B) oscillation is frequently found to be amplitude modulated, with the period of the low-frequency neck (F_N) oscillation.[10] This AM is basically the result of magnetic interaction (MI) but, as we show below, AM may be produced by several contributing mechanisms.

Phillips and Gold[12] have shown that the highly nonlinear nature of MI in the dHvA effect causes a single-crystal sample to behave like a "mixer," generating combination tones ($F_B \pm F_N$). Beating of these sum and difference frequencies could then produce an apparent AM effect. We have found that AM can be observed quite generally over a wide range of magnetic field and temperature and in dilute alloys as well as in pure metals. However, in a few cases we have analyzed the observed amplitude-modulated belly waveform as if it were the resultant of two separate components, for the purpose of making scattering-temperature plots [of $\ln(AH^{1/2})$ vs $(1/H)$]. The result was that the plots for the two components generally had the same slope, within experimental error, so that it did not appear that the AM observed in these cases arose from either a beating of the belly frequency F_B with combination tones $F_B \pm F_N$ (using standard

results of MI theory[12]), or from amplitude modulation of F_B by a factor proportional to the neck amplitude.

Shoenberg and Vuillemin[11] have observed the AM due to MI between the ⟨111⟩ neck and belly frequencies in Au using the field-modulation technique. However, their experiments were restricted to the case of very small modulation amplitude with detection at the fundamental ($n = 1$). They observed both the frequency modulation of the belly frequency and its AM, due to magnetic interaction with the neck-magnetization oscillation. However, they reported that the observed AM was much stronger than is predicted by MI theory (even in the weak MI limit) and was also sensitive to adjustments of the experimental conditions, apparently including the precise adjustment of the current through a coil used to "straighten" the superconducting magnet's magnetic field profile. Furthermore, the belly amplitude was always maximum (minimum) for the biggest positive (negative) swing of $\partial M_N/\partial H$ for the neck, regardless of such changes in experimental conditions. They suggested that some form of phase smearing could perhaps account for the stronger than expected AM, because of the simultaneous FM effect.

Hornfeldt, Ketterson, and Windmiller[13] (hereafter referred to as HKW) have suggested in a recent paper that an applied magnetic field inhomogeneity ΔH (assumed to be linear over the length of the sample) should cause AM through a phase-smearing process. Since the electrons respond to the magnetic induction B, it is the inhomogeneity ΔB which determines the reduction of dHvA amplitude due to phase smearing. However, ΔB can be periodically modulated by the dHvA magnetization oscillations themselves (assumed here to be dominated by a low-frequency signal M_N) such that

$$\Delta B = \left(1 + 4\pi \frac{\partial M_N}{\partial H}\right)\Delta H \,. \tag{1}$$

Thus, AM could arise because any *applied* field inhomogeneity will be *periodically modulated* by the sample's own oscillatory magnetization, with a consequent *periodic variation* of the well-known factor describing the reduction of belly dHvA amplitude due to phase smearing[10] in a *static* inhomogeneous magnetic induction.

In summary, it is known through the experimental work of Shoenberg, Phillips and Gold and others, that a variety of (presumably) *pure* MI effects (not involving magnetic field inhomogeneity or the experimental techniques) can cause AM. In this paper we report detailed observations of two new mechanisms by which MI can lead to AM of high-frequency dHvA oscillations: (i) MI in an inhomogeneous magnetic field (essentially as predicted by HKW); (ii) AM occurring in conjunction with frequency modulation, when the field-modulation technique is used(FM-AM effect). This latter mechanism does not result simply from an extension of the Lifshitz-Kosevitch theory to explicity include MI effects, but is a consequence of the use of the field-modulation technique to observe the dHvA effect. In many cases this FM-AM effect is the *dominant* source of AM and is in any case an unavoidable consequence of using the *large* amplitude field-modulation technique in the presence of appreciable MI.

In Sec. II we describe the way in which AM can arise from MI via the field-modulation and field-inhomogeneity mechanisms. In Sec. III we describe the experimental data-taking arrangements, while Sec. IV contains detailed observations and discussion of the AM resulting from each mechanism.

II. MECHANISMS FOR AMPLITUDE MODULATION

A. FM-AM Effect

We consider a magnetic field orientation for which two dHvA frequencies are present: a high frequency F_B and a low frequency F_N (for example, the ⟨111⟩ belly and neck oscillations in the noble metals). We also assume, for the present, that the sample's oscillatory magnetization $\vec{M}$ is dominated by the contribution $\vec{M}_N$ of F_N. If the amplitude of $\vec{M}_N$ is comparable to the period $P_B (= H^2/F_B)$, of the high-frequency oscillation, then, because the electrons in a metal respond to changes in the magnetic induction $\vec{B}$, and not the field intensity $\vec{H}$, both the magnetic induction

$$\vec{B} = \vec{H}_a + 4\pi\vec{M}_N \tag{2}$$

and the phase of F_B,

$$\phi_B = \left(\frac{2\pi}{P_B}\right)B = \left(\frac{2\pi}{P_B}\right)(H_a + 4\pi M_N) \,, \tag{3}$$

become *oscillatory* functions of the applied field $\vec{H}_a$. This magnetic interaction effect can produce a periodic *frequency modulation* (FM) of the fast oscillation, with the period of the slow oscillation, $P_N = H^2/F_N$, as was first observed by Shoenberg and Vuillemin[11] for the ⟨111⟩ belly and neck in Au. This result follows directly since, when the applied field is changed by an amount ΔH, the corresponding change in magnetic induction ΔB is

$$\Delta B = \left(1 + 4\pi \frac{\partial M_N}{\partial H}\right)\Delta H = (1 + a_N)\Delta H \,. \tag{4}$$

Over any *integral* number of neck cycles $\Delta B = \Delta H$. However, within the period of a single neck oscillation $\Delta B \neq \Delta H$, and the belly dHvA frequency observed as a function of H (or of $1/H$) is an *oscillatory* function of H, being frequency modulated between the limits

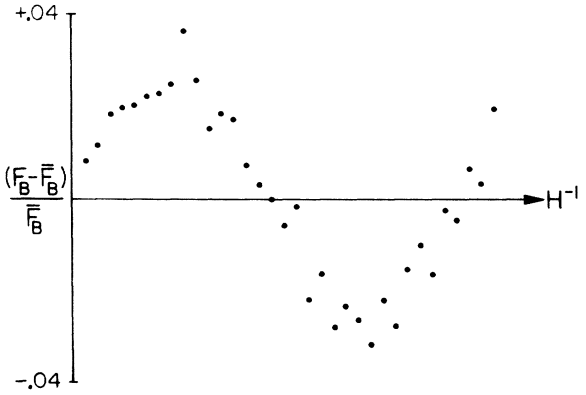

FIG. 1. Plot of $(F_B-\bar{F}_B)/\bar{F}_B$, the fractional difference between the local ⟨111⟩ belly frequency and the average ⟨111⟩ belly frequency, over approximately one cycle of the ⟨111⟩ neck oscillation. The amplitude of the belly frequency modulation is 4π times the absolute neck differential magnetization [Eq. (5)] and agrees with the Lifshitz-Kosevitch theory within experimental error (Ref. 14). The local belly frequency was determined by measuring (by computer) the distance between successive zero crossings of the belly oscillation.

$$F_B^{\pm}=(1\pm|a_N|)F_B^0 \quad , \tag{5}$$

where F_B^0 is the (constant) frequency of the belly oscillation as a function of $\vec{B}$. F_B^0 may be measured as the average of the observed F_B over a large integral number of neck cycles, or as the observed value of F_B near the extrema of M_N, where $a_N=0$. Thus, the extrema of frequency modulation, $F_B^{\pm}$, occur at the positive- and negative-going zero crossings of M_N, where the differential neck magnetization a_N is largest. From (4) it follows also that P_B, the belly period observed vs H, is related to P_B^0, the (constant) period vs B, by

$$P_B=P_B^0/(1+a_N) \ . \tag{6}$$

We have observed and precisely measured the frequency modulation (FM) of the ⟨111⟩ belly by the ⟨111⟩ neck in Au at 2.0 K and 36.1 kG (Fig. 1). We have also used this frequency modulation as a check on independent measurements of the ⟨111⟩ neck dHvA absolute amplitude.[14] Similar measurements of FM have also been made by Shoenberg and Vuillemin.[11]

However, the most dramatic consequence of MI is that, *if the field-modulation technique is used* to observe the dHvA effect, then MI leads directly to a strong periodic *amplitude modulation* (AM) *of the high-frequency oscillation*, with the period of the low-frequency oscillation. Figure 2 shows an example of the AM which was observed for the ⟨111⟩ belly orbit in Au when the dHvA effect was detected simultaneously at seven different even harmonics of the modulation frequency, in a completely *homogeneous* applied magnetic field. The ⟨111⟩ belly amplitude is amplitude modulated with the periodicity of the ⟨111⟩ neck oscillation. However, the depth of AM is strongly dependent on both the detection harmonic number and on the modulation field amplitude. Thus, the mechanism for this form of AM is connected with the field-modulation technique, rather than the dHvA effect *per se*.

This AM arises because the nth harmonic signal detected using the field-modulation technique is proportional to the nth-order Bessel function $J_n(x)$, where $x=2\pi F_B h/H^2$, h is the modulation field amplitude, and F_B is the variable (as a function of H) belly dHvA frequency. According to (5), a value of $a_N=0.1$ will cause a $\pm 10\%$ swing Δx in the argument x of J_n. In our series of experiments the swing ΔF_B for the ⟨111⟩ belly was of order ± 3–4% (Fig. 1). Thus, this "Bessel-function modulation" can in many cases be the dominant source of the experimentally observed total AM and is, in any case, an *unavoidable* consequence of using the large-amplitude field-modulation technique in the presence of appreciable magnetic interaction ($a_N \sim 0.1$).

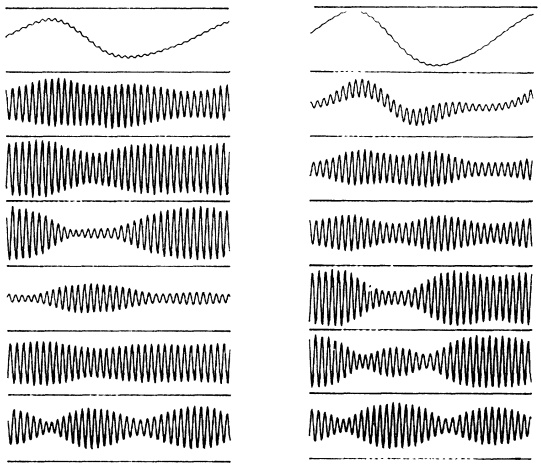

FIG. 2. Amplitude modulation of the ⟨111⟩ belly oscillation, arising from frequency modulation of Bessel-function arguments by magnetic interaction with the ⟨111⟩ neck (FM-AM effect). The data was obtained at $H=36.1$ kG and $T=2.0$ K in a completely homogeneous field ($V\lesssim 0.1$). Results are shown for the even detection harmonics $n=2$–14, for modulation amplitudes $\bar{h}=0.159$ (left side of figure) and 0.318 (right side) in experimental units. The approximate correspondence between $\bar{h}$ and Bessel-function argument $\bar{x}$ is $\bar{x}\simeq 130\,\bar{h}$. However, for quantitative work it is necessary to experimentally measure the actual "modified Bessel-function" factors, which differ slightly from true Bessel functions owing to the finite sample skin depth. The signals detected at the various harmonics have been scaled in amplitude, relative to each other, for presentation here.

It is useful to derive directly the way in which MI modulates both the Bessel-function argument and the observed dHvA frequency, leading to AM and FM, respectively, when using the field-modulation technique. We assume that the oscillatory magnetization is dominated by the Lifshitz-Kosevitch (LK) fundamental ($r=1$) terms (assuming that the amplitudes of the LK harmonics are small compared with the LK fundamental, for each extremal orbit). For completeness we now also explicitly consider the contributions of both the belly and neck orbits to the oscillatory magnetization

$$\vec{M}=\vec{A}_B(H,T)\sin(2\pi F_B^0/B+\phi_B)+\vec{A}_N(H,T)\sin(2\pi F_N^0/B+\phi_N)\ , \tag{7}$$

in which F_B^0 and F_N^0 are the (constant) belly and neck dHvA frequencies and ϕ_B and ϕ_N the corresponding phase factors. (The factors $\vec{A}_B$ and $\vec{A}_N$ are proportional to F_B and F_N but are not frequency modulated because the change from H to B must be made in the expression for M, not in the original free-energy formula.) The magnetic induction $\vec{B}=\vec{H}_a+4\pi\vec{M}=(\vec{H}_0+\vec{h}\cos\omega t)+4\pi(\vec{M}_N+\vec{M}_B)$ is the sum of the applied field $\vec{H}_a$ (dc field plus modulation field) and the oscillatory magnetization $\vec{M}$, so that (7) is an implicit equation for $\vec{M}$. However, Phillips and Gold[12] have shown that the effect of weak *self*-magnetic interaction (i.e., of the belly magnetization with itself and of the neck magnetization with itself) is primarily to modify the harmonic content of the dHvA waveform but to leave the dHvA fundamental nearly unchanged in amplitude. The effects of *self*-MI on the dHvA neck and belly fundamentals are then completely described by rewriting (7) as

$$\vec{M}=\vec{A}'_B(H,T)\sin(2\pi F_B^0/B_B+\phi'_B)+\vec{A}'_N(H,T)\sin(2\pi F_N^0/B_N+\phi'_N)\ , \tag{8}$$

where now

$$\vec{B}_B=\vec{H}_a+4\pi\vec{M}_N\ ,\quad \vec{B}_N=\vec{H}_a+4\pi\vec{M}_B\ , \tag{9}$$

so that only the MI of each magnetization oscillation with the other remains to be considered. The condition for the step from (7) to (8) to be valid is that both $4\pi|\partial M_N/\partial H|$ and $4\pi|\partial M_B/\partial H|$ are $\ll 1$.

By the usual argument the strongest dependence of $\vec{M}$ on $\vec{H}_a$ comes via the rapid variation of the total dHvA phase for the belly and neck oscillations,

$$\Phi_B=2\pi F_B^0/B_B+\phi'_B\ ,\quad \Phi_N=2\pi F_N^0/B_N+\phi'_N \tag{10}$$

as H_a is varied. However, both $\vec{H}_a$ and $\vec{M}_{B,N}$ now contribute to the *change* in phase as $\vec{H}_a$ is varied,

$$\delta\Phi_B(t)=\vec{\nabla}_{\vec{H}_a}\Phi_B\cdot\delta\vec{H}_a=\vec{\nabla}_{\vec{H}_a}\Phi_B\cdot\vec{h}\cos\omega t\ ,$$
$$=-(2\pi F_B^0/H_0^2)\vec{\nabla}_{\vec{H}_a}B\cdot\vec{h}\cos\omega t\ ,$$
$$=-\left(\frac{2\pi F_B^0 h}{H_0^2}\right)\left(1+4\pi\frac{\partial M_N}{\partial H}\right)\cos\omega t\ ,$$
$$\equiv -x_B\cos\omega t\ , \tag{11}$$

in which

$$x_B\equiv\frac{2\pi F_B^0}{H_0^2}\left(1+4\pi\frac{\partial M_N}{\partial H}\right)h=\frac{2\pi F_B^0}{H_0^2}(1+a_N)h\ , \tag{12}$$

where $a_N=4\pi(\partial M_N/\partial H)$, with expressions completely analogous to (11) and (12) for the variation of neck phase. Thus, the total belly and neck phases,

$$\Phi_B(t)=(2\pi F_B^0/H_0^2+\phi'_B)-x_B\cos\omega t\equiv\Phi_B^0-x_B\cos\omega t \tag{13}$$

$$\Phi_N(t)=(2\pi F_N^0/H_0^2+\phi'_N)-x_N\cos\omega t\equiv\Phi_N^0-x_N\cos\omega t\ , \tag{14}$$

are now time dependent. The voltage detected by a pickup coil in the field-modulation technique is

$$V\propto\frac{dM}{dt}\propto\frac{d}{dt}[A'_B\sin\Phi_B(t)+A'_N\sin\Phi_N(t)] \tag{15}$$

$$\propto\frac{d}{dt}\{A'_B[\sin\Phi_B^0\cos(x_B\cos\omega t)-\cos\Phi_B^0\sin(x_B\cos\omega t)]+A'_N[\sin\Phi_N^0\cos(x_N\cos\omega t)-\cos\Phi_N^0\sin(x_N\cos\omega t)]\} \tag{16}$$

which leads to a convenient time Fourier analysis[15]:

$$V\propto\frac{d}{dt}A'_B\left[\sin\Phi_B^0\left(J_0(x_B)+2\sum_{m=1}^{\infty}(-1)^mJ_{2m}(x_B)\cos m\omega t\right)-\cos\Phi_B^0\left(2\sum_{m=0}^{\infty}(-1)^mJ_{2m+1}(x_B)\cos[(2m+1)\omega t]\right)\right] \tag{17}$$

plus a similar term coming from the neck oscillation. Neglecting the dc term, (17) may be written finally as

$$V\propto 2A'_B\sum_{n=1}^{\infty}n\omega(-1)^n\sin(\Phi_B^0+\tfrac{1}{2}n\pi)J_n(x_B)\sin m\omega t \tag{18}$$

again plus a similar term for the neck.

For the case of detection at the fundamental frequency ($n=1$) and with x_B and $x_N\ll 1$ (the case studied by Shoenberg and Vuillemin) Eq. (18) reduces to

$$V\propto(A'_Bx_B\cos\Phi_B^0+A'_Nx_N\cos\Phi_N^0)\sin\omega t \tag{19}$$

$$\propto\left[\frac{\partial M}{\partial B_B}\frac{\partial B_B}{\partial H}+\frac{\partial M}{\partial B_N}\frac{\partial B_N}{\partial H}\right]\frac{\partial H}{\partial t}\propto\frac{\partial M}{\partial H}\frac{\partial H}{\partial t} \tag{20}$$

as it must. Equation (20) is, aside from notation, the starting point used by Shoenberg and Vuillemin in their study of MI in this special case.

For the case of larger x_B and x_N, and arbitrary detection harmonic n, (18) can be written out as

$$V \propto 2A'_B \sum_{n=1}^{\infty} n\omega(-1)^n \sin\left(\frac{2\pi F_B^0}{H_0 + 4\pi M_N} + \phi'_B + \tfrac{1}{2}n\pi\right)$$

$$\times J_n\left(\frac{2\pi F_B^0 h}{H_0^2}(1+a_N)\right) \sin n\omega t \qquad (21)$$

plus a similar expression coming from the neck oscillation. Equation (21) correctly displays both the origin of FM (via MI in the sine term) and the origin of AM via MI modulation of the Bessel-function arguments. Thus, this type of AM arises via MI just as if it were due to actual FM within the Bessel-function arguments. However, as the above derivation shows, the AM actually arises because the belly phase depends directly on the applied field $\vec{H}_a$, but also indirectly via MI, through the dependence of $\vec{M}_N$ on $\vec{H}_a$. The oscillatory magnetization $\vec{M}_N$ can be thought of as alternatively aiding and opposing the applied field $\vec{H}_0$, producing the extremes of FM at the zero crossings of $\vec{M}_N$, where $\partial\vec{M}_N/\partial H$ is largest.

It should be noted that Eq. (11) is an approximation in that only the leading (linear) term in h was kept from the expansion of $\Phi_B(t)$. The largest higher-order terms are of order $(2\pi/P_N)^2 hM_N$ relative to this term, so that the above derivation of the origin of AM of the belly oscillation is quantitatively (as well as qualitatively) correct so long as $hM_N(2\pi/P_N)^2 \ll 1$. Under our experimental conditions ($H = 36.1$ kG and $T = 2.0$ K) $4\pi|\partial M_N/\partial H| \simeq 0.03_5$, $4\pi|\partial M_B/\partial H| \simeq 0.1$ and $hM_N(2\pi/P_N)^2 < 10^{-2}$ if we take $h = 0.1$ in experimental units (see below and Fig. 2 caption). Thus, the description above should be quantitatively correct for the large modulation amplitudes used in our experiments.

B. Effect of Inhomogeneous Applied Magnetic Field

The effect of a *static* inhomogeneous magnetic field in reducing the amplitude of the dHvA oscillations observed from a single-crystal sample has been discussed both by Shoenberg[10] and by HKW.[13] Any variation in magnetic field intensity over dimensions of the sample causes the phase $(2\pi F/H)$ of the dHvA oscillations to differ in different parts of the sample, and the observed dHvA signal, obtained by summing over the entire volume of the crystal, is then reduced by this phase smearing. The factor I, describing the amplitude reduction, generally has the form of a diffractionlike integral. HKW have shown that for a right-circular-cylindrical crystal with its long axis parallel to $\vec{H}$ and also lying along a crystallographic direction for which $\partial F/\partial\theta = 0$ (i.e., a turning point of the dHvA frequency), this factor is

$$I = (\sin\pi V)/\pi V\ , \quad V = \Delta B/P\ , \qquad (22)$$

where both the magnetization of the sample ($\vec{B} \neq \vec{H}$) and its finite demagnetizing factor have been neglected. ΔB is the magnitude of a linear inhomogeneity in the magnetic induction over the sample length and P is the period ($= H^2/F$) of the dHvA oscillation. This expression also holds for a long prism of square cross section (within the same limitations) and is illustrated in Fig. 3. Thus, the amplitude reduction, for this mechanism, is governed solely by the *ratio* of induction inhomogeneity ΔB to the period P of the oscillation.

Equation (22) contains ΔB, rather than ΔH_a, since the conduction electrons in a metal respond to the magnetic induction $\vec{B}$, and not just the applied field intensity, $\vec{H}_a$. Substituting (1) in (22), the periodic modulation of ΔB should give rise to a periodic modulation of the amplitude reduction factor I in (22). If we again consider the case of a crystal orientation for which high-frequency, F_B, and low-frequency, F_N, dHvA oscillations are simultaneously present, and consider values of field and temperature such that $\partial M/\partial H$ is dominated by the low-frequency oscillation (as for the ⟨111⟩ direction in the noble metals), HKW predict that the measured amplitude of the *high-frequency* oscillation F_B will be *amplitude modulated* (AM) at the low frequency F_N, as soon as $\Delta H \neq 0$, via modulation of the argument, $V = (\Delta B/P_B)$, of I, as shown in Fig. 3. Thus, the source of this AM is magnetic interaction and phase smearing in an inhomogeneous applied field.

It is useful, for comparison later with our experimental results, to point out here the predicted variation of this AM with progressively increasing field inhomogeneity ΔH (see Fig. 3): (i) essentially *no* AM in a homogeneous field ($V \lesssim 0.1$); (ii) large AM as ΔH is increased to approach $V = 1.0$ ($\Delta H \approx P_B$, and taking $4\pi(\partial M_N/\partial H) \lesssim 0.1$); (iii) *decreasing*

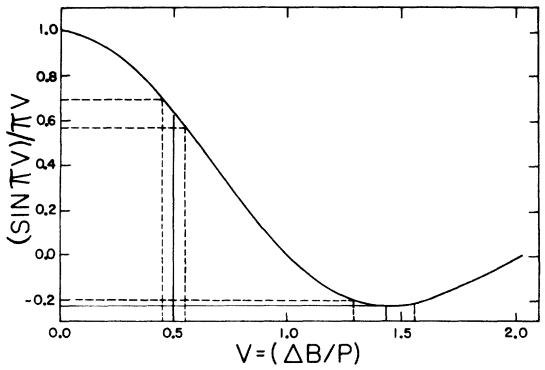

FIG. 3. Factor $I = (\sin\pi V)/\pi V$, describing the phase-smearing reduction in dHvA amplitude due to field inhomogeneity, as calculated by HKW[13] under the conditions described in the text. Two examples of the amplitude modulation resulting from magnetic interaction in two different linear field gradients are also shown, taking $4\pi(\partial M/\partial H) = 0.1$. For $V = 0.5$ the AM is ±10%, while for $V = 1.43$ the AM is ±5%.

AM as ΔH is *increased further*, approaching *no* AM at $V \simeq 1.43$.

III. EXPERIMENTAL TECHNIQUES

Since crystals of pure Au, with the magnetic field along the ⟨111⟩ direction, are particularly convenient for the observation of interaction effects between a high-frequency (belly) and a low-frequency (neck) dHvA oscillation. All of the Fermi-surface parameters needed to calculate the noninteracting amplitudes of $a_N = 4\pi(\partial M_N/\partial H)$ and $a_B = 4\pi(\partial M_B/\partial H)$ from the Lifshitz-Kosevitch theory are now known with an accuracy of (at worst) a few percent, while the small neck effective mass (0.28) permits relatively large values of a_N to be obtained with only modest requirements on magnetic field and temperature.

The Au sample used in these experiments was spark-cut from a larger single crystal ingot which was grown in a boron nitride crucible by the Bridgman technique and cooled slowly to room temperature. The sample, a prism with square cross section ~1.1 mm on a side and ~6.6 mm long (and with ⟨111⟩ along the long axis) was heavily etched with aqua regia before mounting in a nearly strain-free way in a small-angle rotator. The dHvA oscillations were used to orient the ⟨111⟩ axis along the field direction with an accuracy ~0.05°. The etched sample was scanned optically and with x rays before the experiments; the low neck Dingle temperature, which rose from 0.2 to 0.45 K in the course of three separate experiments using this sample, strongly indicates that a high degree of physical sample perfection and nearly strain-free mounting was achieved. The long, thin sample geometry was chosen for convenience in establishing known linear field gradients over the sample length and to minimize the effect of internal demagnetizing fields.

The field-modulation technique was employed, together with a computer-centered automated digital system.[16] The data-taking arrangements were as follows:

(i) All data on the effect of field inhomogeneity were obtained at 2.02 K with the superconducting solenoid set at 36.1 kG. The belly period is only 2.90 G at this field and so, to obtain a high-resolution field sweep, the superconducting magnet was put into its persistent mode and the field was digitally swept proportional to $1/H$ through 256 steps, covering a window of ~100 G, using a pair of coils in the bore of the magnet. In this way the (arbitrarily established) absolute phase of data sets taken on successive field sweeps, but at different modulation field amplitudes and with different applied-field gradients, could be approximately preserved and the resulting amplitude-modulation effects could be compared directly (see below).

(ii) A software phase-sensitive detector was used to simultaneously detect the two quadrature components of the magnetization oscillations at the first seven even harmonics of the field-modulation frequency (~98 Hz). A fast analog-to-digital converter was used to digitize data while a laboratory computer with a magnetic disk was used for data file storage.[16]

Thus, a typical "data window," at any given detection harmonic, contains 256 data points spanning ~35 belly cycles and slightly more than one neck oscillation cycle ($F_B/F_N = 29.33$). In addition to allowing us to explore detection harmonic-dependent amplitude-modulation effects, simultaneous detection at more than one harmonic provided a check for the presence of skin depth effects,[16] and verification that AM due to magnetic field inhomogeneity was independent of the detection harmonic number.

(iii) The Bessel functions $J_n(x)$, which appear as factors in the observed dHvA amplitudes when using the field-modulation technique, were determined experimentally by stepping the modulation field amplitude from zero to the maximum available from our modulation coil, and measuring the amplitude of the detected signal at each step. This was done for all even harmonics, $n = 4$ through 14 and is necessary because the experimental "Bessel functions" differ slightly from true Bessel functions.[17]

(iv) The magnetic field profile was measured using a bridge and a Bi magnetoresistor mounted above the sample. (The sample probe was displaced to make a profile measurement.) The field profile was corrected to second order (by computer) and a linear field gradient produced over the sample, by adjusting the currents in a "curvature" coil (simple short solenoid) and a "slope" coil (two short solenoids connected in opposition and spaced coaxially ~3 cm apart). Field differences could be measured with a precision ~0.1 G and linear gradients ranging from ~0.3 to ~4.0 G, over the sample length, were produced. However, a series of time-consuming attempts were generally needed to produce any particular field gradient. This fact, together with small residual uncertainties in the sample position, made necessary a compromise between the absolute accuracy with which desired gradients could be produced over the sample length, and the precision with which individual field differences could be measured. Figure 4 shows a typical final magnetic field profile obtained in this way.

IV. RESULTS

A. FM-AM Effect

As was shown in Sec. II, MI of the ⟨111⟩ neck magnetization on the ⟨111⟩ belly oscillations leads

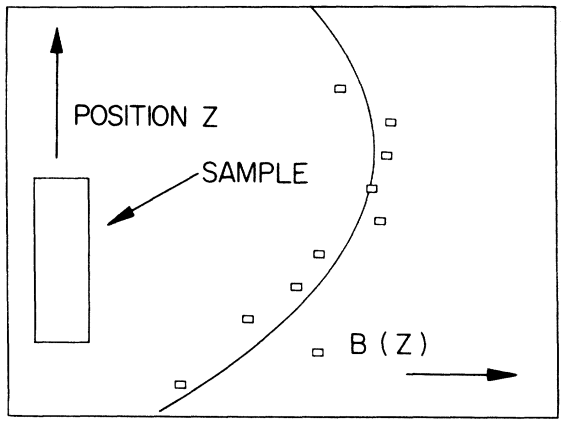

FIG. 4. Magnetic field profile (abscissa) vs position (ordinate) at $H \simeq 36.1$ kG. The position of the 6.6 mm long sample is shown; the total field difference between the left and right borders of the figure is 1 G. Experimental field values are shown (□), along with a second-order computer fit to the points; the fitted curve was used to calculate correction currents for the gradient and curvature coils, in order to produce a linear field gradient over the sample dimensions.

directly to amplitude modulation of the belly oscillation, via modulation of the arguments of the nth-order Bessel functions which are factors in the observed belly amplitude. In practice one can very conveniently observe AM of the high-frequency belly oscillation by fixing the modulation field amplitude for operation near some mean Bessel argument $\bar{x}$, and then simultaneously detecting the ⟨111⟩ belly dHvA amplitude at a sequence of detection harmonics, n. In general, the depth of AM, m, resulting from FM, for any particular detection harmonic n, will be

$$m = \frac{A_{\max} - A_{\min}}{A_{\max} + A_{\min}} = \frac{J_n(\bar{x} + \Delta x) - J_n(\bar{x} - \Delta x)}{J_n(\bar{x} + \Delta x) + J_n(\bar{x} - \Delta x)} \quad . \tag{23}$$

If x is chosen such that $J_n'(x) \neq 0$ then

$$m \simeq \frac{J_n'(\bar{x})}{J_n(\bar{x})} \Delta x = \frac{J_n'(\bar{x})}{J_n(\bar{x})} \quad \frac{\Delta x}{\bar{x}} \quad \bar{x} \ , \tag{24}$$

in which $\Delta x = 2\pi \Delta F_B h / H^2 = a_N \bar{x}$ is the maximum swing of the Bessel argument. For small MI (small a_N) the resulting AM is then proportional (i) to a_N, (ii) to the mean Bessel argument $\bar{x}$ and (iii) to the slope of the nth-order Bessel function near the operating point. If the modulation amplitude is fixed then the resulting AM depends primarily on the rate of variation of the nth-order Bessel function near the operating point.

Table I illustrates the fact that the condition for large AM, via the FM-AM effect, is the same as that for large FM: $a_N = 4\pi(\partial M_N / \partial H)$ should be appreciable (0.1–0.3 suffices) in which case this

TABLE I. Amplitude modulation $m = (A_{\max} - A_{\min})/(A_{\max} + A_{\min})$ of a high-frequency dHvA oscillation, resulting from modulation of the Bessel-function argument by magnetic interaction with a low-frequency oscillation $[a_N = 4\pi\ (\partial M_N/\partial H)]$, when detection is tuned for the first peak of J_n ($n = 2$, 4, 6, 8, 10) using the field-modulation technique.

	m (%)				
a_N	$n=2$	4	6	8	10
0.035	0	±1	±1	±1	±1
0.1	±1	±3	±6	±10	±13
0.2	±6	±14	±27	±47	±67
0.5	±43	zc[a]	zc	zc	zc

[a]zc Bessel-function zero crossing, corresponding to ±100% amplitude modulation due to FM.

mechanism for AM is unavoidable, even with the modulation amplitude tuned for detection at the first peak of a Bessel function (in which case $J_n''(x)$, and higher derivatives, govern the extent of AM).

The AM due to modulation of Bessel function arguments is much larger than that given by Table I when detecting *away* from a Bessel peak. Figures 5–7 and Table II compare the AM observed for h

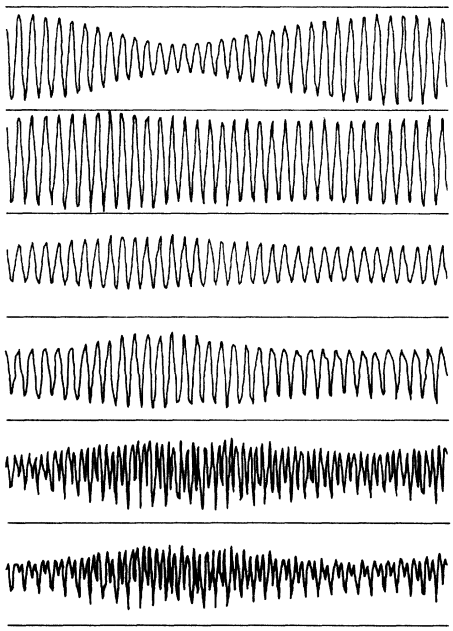

FIG. 5. FM-AM effect at 2.0 K and 36.1 kG in a completely homogeneous field ($V \lesssim 0.1$) for the even detection harmonics $n = 4$–14. The modulation amplitude $\bar{h} = 0.059$ (experimental units), corresponding to a location just beyond the first peak of the J_6 Bessel function (see Fig. 7). The AM measured at each detection harmonic is compared in Table II with that calculated using each measured Bessel function at the operating point $\bar{h}$ together with the observed belly FM.

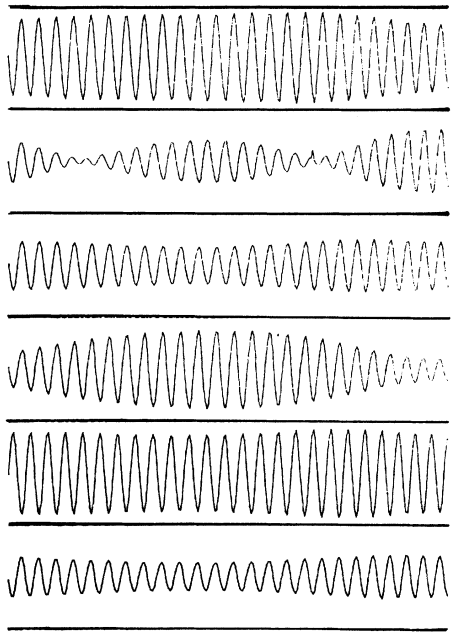

FIG. 6. FM-AM effect at 2.0 K and 36.1 kG in a linear field gradient, $V \leq 1.4$, for the even detection harmonics $n=4$–14. This value of V corresponds to the first negative peak of $(\sin \pi V)/\pi V$, so that the AM observed is due entirely to the FM-AM effect and not to field inhomogeneity. The modulation amplitude is $\bar{h}=0.111$ (experimental units), corresponding to a location at the first peak of the J_{12} Bessel function (see Figure 7). The AM measured at each detection harmonic is compared in Table II with that calculated using each measured Bessel function at the operating point $\bar{h}$ together with the observed belly FM.

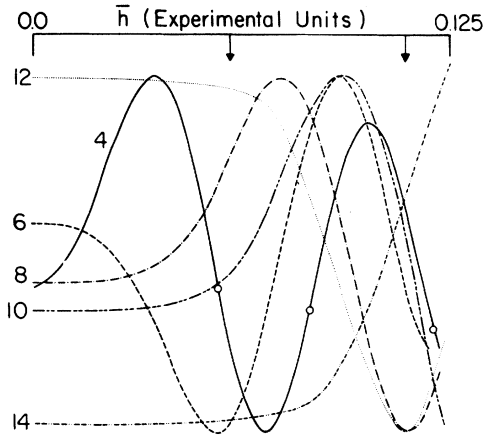

FIG. 7. The experimentally measured "Bessel functions" J_4 through J_{14}. The plots were produced by measuring the detected dHvA amplitude at each even detection harmonic as the modulation amplitude h was stepped from 0 to approximately 0.125 (experimental units). The operating points for the data of Figs. 5 and 6 are indicated by arrows. A shift of the zero crossing line was also observed for J_4; the zero crossings for J_4 are indicated by open circles.

$=0.059$ and 0.111 (in experimental units) with the AM which was calculated directly from the measured Bessel functions (Fig. 7) at these two operating points, using FM of $3\frac{1}{2}\%$ for the calculation.

If the mean Bessel argument $\bar{x}$ is sufficiently large, then the resulting AM at successive detection harmonics may appear qualitatively very different, depending on whether the operating point is near a Bessel peak or zero crossing, or on a region of positive or negative Bessel slope. As Fig. 8 shows, the maximum of the amplitude-modulating envelope of the belly dHvA waveform may occur at either the maximum or minimum of $4\pi(\partial M_N/\partial H)$, depending on the slope of the Bessel function at the operating point. The AM may also appear to occur at twice the neck frequency, for operation near a Bessel peak.

If the Bessel argument is sufficiently large that the operating point is several peaks out on a low-order Bessel function, then FM of only a few percent can sweep the operating point from a Bessel peak clear through a zero crossing, resulting in AM greater than 100%. Figure 2 shows examples of this extreme AM for two successively larger modulation levels. Another example of large AM resulting from operation near a Bessel zero crossing is apparent for $n=6$ in Fig. 6.

The AM arising out of FM is also of interest in the opposite extreme of very small Bessel arguments [$x \ll$ first peak of $J_n(x)$]. Since $J_n(x)$ rises as x^n in this limit, any FM is nonlinearly amplified in the resulting AM: a $\pm 10\%$ FM of x should produce $\pm(10n)\%$ AM. As Fig. 5 and Table II show, the AM observed for $\bar{x}=0.059$ and $n=10$, 12, 14 does increase approximately as $(n+2)/n$ for successive even detection harmonics. For $n=4$, 6, 8 and $\bar{x}=0.024$, amplitude modulations of $\pm 16\%$, $\pm 27\%$ and $\pm 39\%$ were measured, again increasing

TABLE II. Comparison of the observed and the predicted AM due to FM for two different Bessel-function operating points ($\bar{h}=0.059$, 0.111) and for even detection harmonics ($n=4$–14). The observations are taken from the data of Figs. 5 and 6. The calculated AM was obtained using a FM of $\pm 3\frac{1}{2}\%$ and the measured Bessel functions shown in Figure 7.

	$\bar{h}=0.059$		$\bar{h}=0.111$	
n	Observed (%)	Calculated (%)	Observed (%)	Calculated (%)
4	±50	±55	±14	±26
6	±9	±6	±75(zc)[a]	zc[a]
8	±19	±11	±17	±14
10	±22	±18	±61	±58
12	±24	±22	±7	±3
14	±32	±26	±20	±18

[a]zc Bessel-function zero crossing, corresponding to $\pm 100\%$ amplitude modulation due to FM.

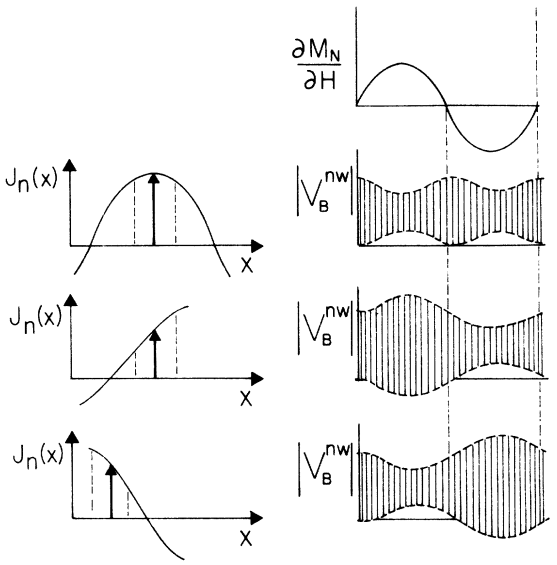

FIG. 8. The figure illustrates that the maximum (minimum) of the amplitude modulated envelope for the belly oscillations, due to the FM-AM effect, occurs at the maximum of $\partial M_N/\partial H$ when the operating point $\bar{x}$ corresponds to a region of positive (negative) Bessel function slope. If $\bar{x}$ corresponds to a Bessel peak, then the AM occurs at twice the neck frequency.

proportional to $(n+2)/n$, as expected from the x^n behavior of $J_n(x)$ for small arguments.

B. Effect of Field Inhomogeneity

Data were taken for five different values of linear applied field inhomogeneity, at several modulation-field amplitudes, and at seven different even detection harmonics, $n = 2-14$. Figure 9 contains our results showing the effect of progressively larger linear magnetic field gradients on the ⟨111⟩ belly amplitude, in the presence of (weak) magnetic interaction with the ⟨111⟩ neck oscillation. Increasingly deep amplitude modulation (AM) is clearly present as V is increased from 0.1 to 0.8; when ΔH is further increased to $V = 1.38$ the AM nearly disappears.

The results for detection at 2ω or 6ω ($\omega/2\pi \sim 98$ Hz) are virtually identical, where the modulation field amplitude has been adjusted in each case to be near (but not quite on) the first peak of the J_2 and J_6 Bessel functions, respectively. By increasing the modulation field amplitude the ⟨111⟩ neck oscillation can be detected by itself. Doing this while keeping the magnet in the persistent mode and keeping the field gradient unchanged, and then comparing the recordings of ⟨111⟩ neck and belly oscillations, we find that the maximum and minimum of the belly AM do occur at the zero crossings of M_N; i.e., at the extrema of $\partial M_N/\partial H$. The observed behavior of the AM is thus in qualitative agreement with the prediction by HKW, the observed decrease of AM (at $V = 1.38$) corresponding to arrival near the first negative peak of $(\sin\pi V)/\pi V$, which should occur at $V = 1.43$.

The FM-AM effect, described above, is responsible for the fact that the observed AM does not vanish in either a homogeneous field ($V = 0$) or near $V = 1.43$ (see Figure 9). As described above, the FM-AM effect may be minimized by choosing x so as to operate at a local Bessel-function extremum, where $J_n'(x) = 0$, but if the FM is appreciable there will still be a significant AM contribution at such an extremum. In these experiments ΔF_B was $\pm 3.5\%$ [$a_N = 4\pi(\partial M_N/\partial H) = 0.035$]. For the data reported here, the modulation amplitude happened to be such that the Bessel function had a slightly negative slope for J_2 and J_6 (operating just beyond the first maximum of each at $x = 0.024$ and 0.059, in the experimental units of Fig. 7). Under these conditions the inhomogeneity AM and the FM-induced AM are additive as a function of $4\pi(\partial M_N/\partial H)$, but the FM contribution is near minimal. It

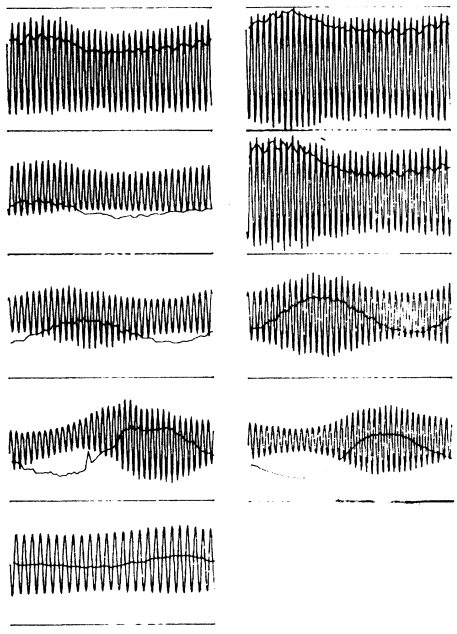

FIG. 9. Effect of applied magnetic field inhomogeneity on the depth of amplitude modulation of the ⟨111⟩ belly by the ⟨111⟩ neck in Au at 36.1 kG and 2.0 K. On the left are results obtained with 2ω detection, on the right with 6ω detection (ω = field-modulation frequency). The values of V [field inhomogeneity parameter, Eq. (22)] are (reading down from the top): 0.07, 0.3, 0.6, 0.8, 1.38. The distance from the bottom border of each figure to the wavy line running through each set of oscillations gives the local peak-to-peak amplitude of the belly oscillation (in arbitrary units).

TABLE III. Observed, corrected, and predicted values of the depth of amplitude modulation of the ⟨111⟩ belly by the ⟨111⟩ neck in Au, due to magnetic interaction in an inhomogeneous magnetic field, as described in the text.

	Observed m(%)		Corrected m(%)[a]		Calculated m(%)[b]	
V	$n=2$	6	2	6	$a_N=0.035$	$a_N=0.10$
0.07	±9	±7	±1	±1	0	0
0.3	±18	±16	±8	±10	±1	±3
0.6	±24	±27	±14	±21	±5	±16
0.8	±48	±48	±38	±42	±16	±45
1.38	±9	•••[c]	±1	•••[c]	±2	±9

[a]Corrected for the AM due to the FM-AM effect (see text).

[b]Using Eqs. (1) and (22), from HKW (Ref. 13).

[c]No AM measurement was made with the modulation amplitude near the first peak of J_6, for this value of field inhomogeneity ($V=1.38$).

is necessary to correct for the additional AM due to the FM-AM effect, in order to make quantitative comparison with the HKW calculation. These AM corrections are ± 10% at 2ω and ± 6% at 6ω, at our measured Bessel operating points. We again define the depth of AM using Eq. (23), where A is the corrected amplitude for the ⟨111⟩ belly. The results of our measurements of the AM due to field inhomogeneity are presented in Table III, where they are also compared with the predicted AM, calculated from Eqs. (1) and (22) (using $a_N = 0.035$).

As Table III shows, the corrected observed depth of AM is larger than that predicted by HKW, though there is excellent qualitative agreement as a function of $V=\Delta B/P_B$. Several factors make quantitative comparisons difficult, including a finite demagnetizing factor (about 0.1) and the non-second-order surface shape of our sample (which produces an inhomogeneous demagnetizing factor over the volume of the sample). The inhomogeneity of the demagnetizing factor should be most important physically at the high detection harmonics, where the skin depth is small. We do find evidence for skin depth effects in that the measured "Bessel function" zero crossings for high n occur at higher Bessel argument than would be predicted simply by scaling relative to the observed positions of the low-n Bessel zeros and peaks. Any nonuniformity of the effective magnetization should also have the consequence of slightly smearing out zeros of the observed belly dHvA amplitude, thus *reducing* the magnitude m of AM. Since $\vec{M}_N$ varies (slightly) through the sample due to nonuniform demagnetization, then the occurrence of a zero of $\vec{M}_B$ in one part of the sample will not quite correspond to a zero in another region; for a small demagnetizing factor this effect will be important only when $\vec{M}_B$ would otherwise be zero.

C. Discussion and Conclusions

The experiments demonstrate that AM of a high-frequency dHvA oscillation can result either from magnetic interaction with a low-frequency oscillation in an inhomogeneous magnetic field, via phase smearing, or from modulation of Bessel-function arguments, as a result of using the field-modulation technique. The depth of the latter FM-AM effect is in excellent agreement, for different detection harmonics and modulation amplitudes, with calculations based on the observed detection Bessel functions and the measured belly FM. The qualitative behavior of the AM due to field inhomogeneity is also in excellent agreement with the prediction of HKW,[13] particularly in that the AM goes to a minimum near $V=1.43$. However, quantitative agreement is less good, possibly because of the presence of other sources[13] of phase smearing or because of demagnetizing effects.

An understanding of these two AM mechanisms does make it possible to adjust experimental parameters to minimize AM, and to improve the relative precision of a set of dHvA amplitude measurements. For example, if AM arises from the FM-AM effect then *any* set of amplitude measurements at a sequence of magnetic field values can be used in making a Dingle plot to determine the electronic scattering rate, provided that each measurement in the set is made at the same point in phase on the modulating waveform.

Because of the simultaneous presence of the FM-AM effect, the AM due to field inhomogeneity does not seem to provide a reliable method for measuring the *absolute* amplitude of dHvA oscillations, as was suggested by HKW.[13] However, the absolute dHvA amplitude for a low-frequency oscillation can be measured accurately either by waveform analysis,[14] or by measuring the FM of a coexistent high-frequency dHvA oscillation (as in Fig. 1).[11,14] Such measurements of the FM of a high-frequency oscillation may also provide a convenient way of detecting very-low-frequency dHvA oscillations with the field-modulation tech-

nique. The presence of FM also has the incidental consequence that very accurate measurements of the frequency of a high-frequency dHvA oscillation should be made over an integral number of cycles of any coexistent low-frequency oscillation, in order to average out the effect of FM.

ACKNOWLEDGMENTS

We particularly wish to thank Professor D. Schoenberg for his critical reading of the typescript, which resulted in several improvements of the presentation, and for helping to establish the connection between our work and that of Shoenberg and Vuillemin [Eqs. (18)–(20)]. We would like to thank Yun Chung for growing the Au single crystal which was used in these measurements. We wish to express our appreciation to Dr. S. Hornfeldt, Dr. L. Windmiller, Dr. G. Crabtree, and J. Ketterson for discussions which helped to stimulate this work both during and after a visit by one of us (D. H. L.) to Argonne National Laboratory. We also wish to thank Professor R. J. Higgins for the use of measurement facilities constructed by one of us (H. A.) with the support of NSF Grant Nos. GJ-32786 and GH-33775. Finally, D. H. L. gratefully acknowledges support from NSF Grant No. GH-32982.

---

*Research conducted at the University of Oregon with support from the National Science Foundation and the Research Corp.

†Current address: Bell Laboratories, Murray Hill, N. J. 07974.

[1]D. H. Lowndes, K. Miller, R. Poulsen, and M. Springford, Philos. Trans. R. Soc. Lond. A **331,** 497 (1973).

[2]D. H. Lowndes, K. Miller, R. Poulson, and M. Springford, in *Proceedings of the Thirteenth International Conference on Low Temperature Physics, Boulder, Colo., 1972,* edited by R. H. Kropschot and K. D. Timmerhaus (University of Colorado Press, Boulder, Colo., 1973).

[3]M. Springford, Adv. Phys. **20,** 493 (1971).

[4]R. Harris and W. Blaker, J. Phys. C **4,** 569 (1971).

[5]P. T. Coleridge, J. Phys. F **2,** 1016 (1972).

[6]R. J. Higgins and D. W. Terwilliger, Phys. Rev. B **7,** 667 (1973); H. Alles, M. Chang, R. J. Higgins, and D. W. Termilliger, in Ref. 2.

[7]L. F. Chollet and I. M. Templeton, Phys. Rev. **170,** 656 (1968); P. T. Coleridge and I. M. Templeton, Can. J. Phys. **49,** 2449 (1971).

[8]H. R. Brown and A. Myers, J. Phys. F **2,** 683 (1972).

[9]A. Arko and F. M. Mueller, Phys. Rev. Lett. **29,** 1515 (1972).

[10]D. Shoenberg, Philos. Trans. R. Soc. Lond. A **255,** 85 (1962); Phys. Kondens. Mater. **9,** 1 (1969).

[11]D. Shoenberg and J. J. Vuillemin, in *Proceedings of the Tenth International Conference on Low Temperature Physics, Moscow, 1966,* edited by M. P. Malkov (VINITI, Moscow, 1967); D. Shoenberg, Can. J. Phys. **46,** 1915 (1968).

[12]R. A. Phillips and A. V. Gold, Phys. Rev. **178,** 932 (1969).

[13]S. Hornfeldt, J. Ketterson, and L. Windmiller, J. Phys. E **6,** 265 (1973).

[14]H. Alles, D. H. Lowndes, and R. J. Higgins (unpublished).

[15]A. Goldstein, S. J. Williamson, and S. Foner, Rev. Sci. Instrum. **36,** 1356 (1965).

[16]H. Alles, Ph.D. thesis (University of Oregon, 1972) (unpublished).

[17]See the discussion of experimental techniques by A. V. Gold, in *Electrons in Metals* (Gordon and Breach, New York, 1968), Vol. 1, pp. 112–121.